Temperature and intensity dependence of the open-circuit voltage of InGaN/GaN multi-quantum well solar cells

Matthias Auf der Maur[a,*], Gilad Moses[b,c], Jeffrey M. Gordon[b], Xuanqi Huang[d], Yuji Zhao[d] and Eugene A. Katz[b]

[a] *Department of Electronic Engineering, University of Rome Tor Vergata, 00133 Rome, Italy*

[b] *Department of Solar Energy and Environmental Physics, Blaustein Institutes for Desert Research, Ben-Gurion University of the Negev, Sede Boqer Campus, 8499000, Israel*

[c] *Albert Katz School for Desert Studies, Blaustein Institutes for Desert Research, Ben-Gurion University of the Negev, Sede Boqer Campus, 8499000, Israel*

[d] *School of Electrical, Computer and Energy Engineering, Arizona State University, Tempe, AZ 85287, USA*

ARTICLE INFO

Keywords:
Open circuit voltage
InGaN/GaN multi-quantum wells
concentrator photovoltaics
carrier recombination
band gap

ABSTRACT

Motivated by possible application of InGaN/GaN multi-quantum well solar cells in hybrid concentrated photovoltaic-solar thermal power conversion systems, we have analyzed the temperature and intensity dependence of the open-circuit voltage of such devices up to 725 K and more than 1000 suns. We show that the simple ABC model routinely used to analyze the measured quantum efficiency data of InGaN/GaN LEDs can accurately reproduce the temperature and intensity dependence of the measured open-circuit voltage if a temperature-dependent Shockley-Read-Hall lifetime is used and device heating is taken into account.

1. Introduction

In recent years, InGaN/GaN multi-quantum well (MQW) structures have gained increasing interest for photovoltaic (PV) applications [1, 2, 3, 4, 5, 6, 7]. This is principally due to their large absorption coefficient and the tunability of the bandgap of InGaN alloys over the whole visible spectrum. Moreover, their resistance to radiation and their high thermal stability make III-nitrides ideally suited for photovoltaic applications [3, 6, 7]. In particular, recent studies have shown good performance of InGaN/GaN MQW cells at high solar concentration and over a large temperature range [8]. The principal motivating application for our study is incorporating PV devices in hybrid concentrating PV-solar thermal power systems where the solar cell absorber operates at high enough temperatures to drive conventional steam turbines [9]. This is distinct from and unrelated to thermo-photovoltaic power generation where the PV cells are irradiated by an intermediate hot source rather than directly by solar radiation, with the cells maintained at as low a temperature as feasible.

The open-circuit voltage (V_{oc}) is of special importance for concentrated photovoltaics working at high temperatures. While increasing irradiance increases V_{oc}, higher temperatures decrease it [10]. The optimization of solar cell performance therefore requires a full understanding of the dependence of V_{oc} on incident intensity and device temperature T.

V_{oc} is related to the splitting of the electron and hole quasi-Fermi levels, which results from the balance of optical generation rate G and recombination rate R, i.e. $R(n,p) = G$, where n and p are the respective carrier densities. If a single recombination channel dominates and the Boltzmann approximation is valid, then assuming $n = p$ the difference of the quasi Fermi levels and thus V_{oc} is given by [11]

$$V_{\mathrm{oc}} = \frac{E_g}{q} + \frac{\eta k_B T}{q} \ln \frac{G}{C(N_c N_v)^{\frac{1}{\eta}}}. \tag{1}$$

*Corresponding author
auf.der.maur@ing.uniroma2.it (M. Auf der Maur)
ORCID(s): 0000-0002-4815-4485 (M. Auf der Maur)

Here E_g is the band gap energy, k_B the Boltzmann constant, q the elementary charge, C the recombination parameter, and $N_{c,v}$ the electron and hole effective density of states. G is assumed proportional to the incident light intensity. The parameter η is related to the degree of the recombination process and is 2, 1 or 2/3 for Shockley-Read-Hall, radiative and Auger recombination, respectively [11].

V_{oc} is also described by the equivalent diode model [12, 10] as

$$V_{\mathrm{oc}} = \frac{E_g}{q} + \frac{\eta k_B T}{q} \ln \frac{I_{\mathrm{ph}}}{I_0}, \tag{2}$$

where I_0 is the diode saturation current, I_{ph} is the photo-generated current and η is the diode ideality factor. Comparing with (1), the diode ideality factor can be related to the dominant recombination process. Note that η is bias-dependent since the dominant recombination process changes as carrier injection varies. It can be larger than 2 in the presence of other processes such as trap-assisted tunneling [13].

As seen from both models, the temperature and intensity dependence of V_{oc} permit the determination of two important device parameters. The extrapolation to $T = 0$ K should provide E_g independent of G. The derivative of V_{oc} with respect to $\ln G$ at fixed T should yield a constant slope from which the value of η, and hence the dominant recombination mechanism can be deduced. These two quantities can be obtained experimentally by temperature and intensity dependent measurements, respectively.

Such experiments have been performed recently on c-plane InGaN/GaN MQW solar cells [8], revealing discrepancies with the above deductions from the simple analytic models. Specifically, the extrapolated value of qV_{oc} was found to be larger than the E_g extracted from photoluminescence (PL) and external quantum efficiency (EQE) measurements. Moreover, at intensities above ~ 100 suns, the V_{oc} versus $\ln G$ curve changes slope. Figure 1 shows the measured V_{oc} as a function of T for different intensities measured with a fiber-optic minidish solar concentrator [14, 15]. For the lower concentration regime, the data show linear behavior as predicted from the model equations. Linear extrapolations to 0 K at different intensities, indicated by dashed lines in the figure, indeed converge to a single value of $E_g \approx 3.15$ eV. But this is ~ 0.3 eV higher than the E_g extracted from both quantum efficiency and PL measurements, considering the temperature dependence of E_g described by Varshni's law [16], and also with respect to theoretical k·p calculations we performed for this device structure. Similarly, the slope $S = q/k_B T \cdot \partial V_{\mathrm{oc}}/\partial \ln I$ of the V_{oc} versus intensity data shown in Fig. 3 is constant near a value of 2 up to ~ 100 suns, but then drops quickly to below 1. This suggests dominance of defect-related Shockley-Read-Hall (SRH) recombination at lower concentration, but also a transition to other recombination processes, or a thermal effect at higher intensity, or both.

2. Calculation

We will now show that the data are compatible with the ABC model commonly used for the analysis of III-nitride light emitting diodes (LEDs) [17, 18], provided a temperature-dependent SRH parameter and device heating at high intensity are accounted for. In the ABC model, R is given as a sum of three contributions up to third order in the carrier density:

$$R = An + Bn^2 + Cn^3. \tag{3}$$

This model follows from standard recombination models [19] under the assumption of equal electron and hole densities. The first two terms are identified with SRH and radiative recombination, respectively, and the third with Auger recombination, although it might also model carrier leakage [20]. It can be assumed that all recombination in the MQW structure is governed by the quantum well populations, so that n is interpreted as the 2D electron density. We also invoke the Boltzmann approximation, which is justified for the intensities considered here. Furthermore, we identify V_{oc} with the quasi-Fermi level splitting in the MQW region, and assume a homogeneous distribution of generation and recombination over the quantum wells. Then V_{oc} can be obtained in closed form from (3) equating $R = G$ and using formulas for solving cubic equations [21]. This leads to

$$\Delta_0 = B^2 - 3AC,\ \Delta_1 = 2B^3 - 9ABC - 27C^2G,$$

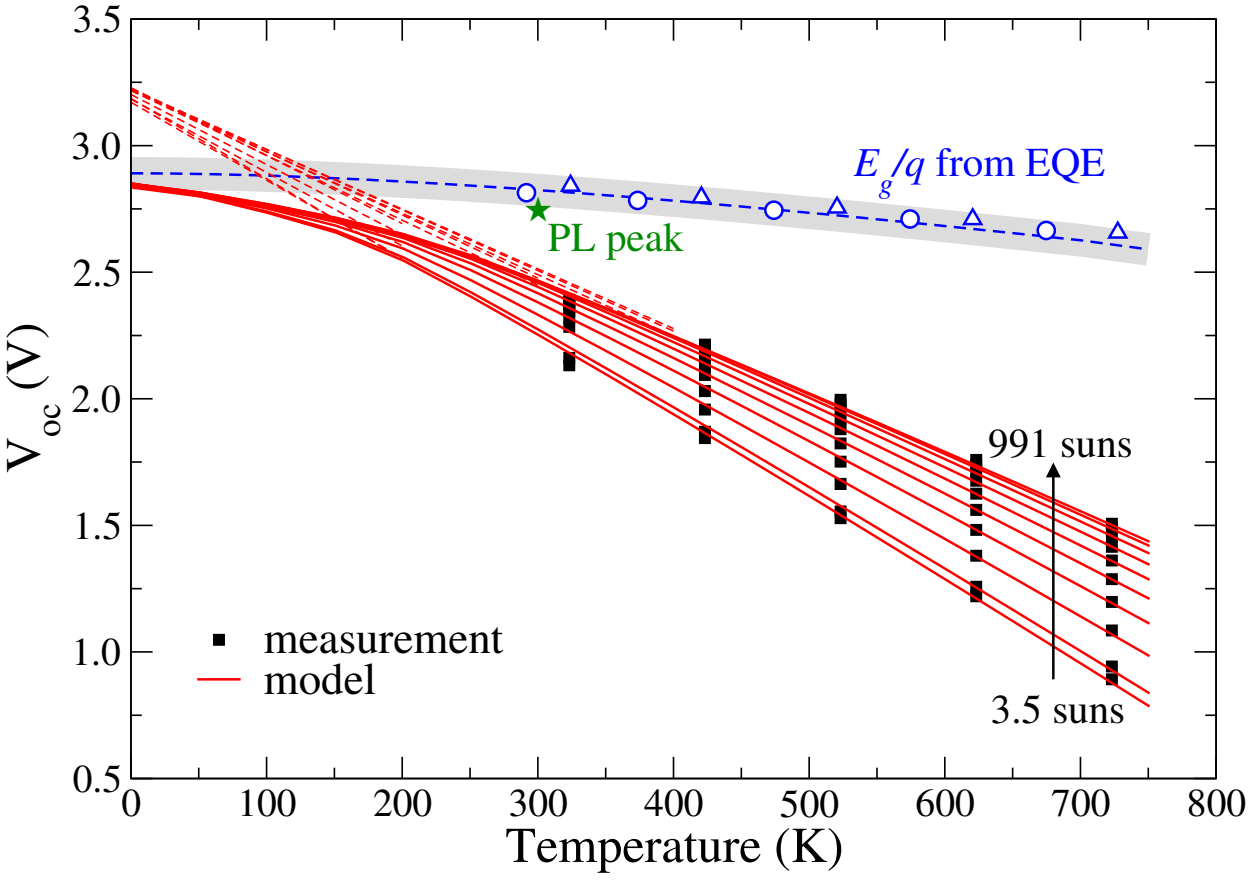

Figure 1: V_{oc} versus temperature T for the studied InGaN/GaN MQW solar cell. The black squares are measured values for different intensities from 3.5 – 991 suns. E_g/q estimated from the EQE (blue open symbols) and PL (green star) data is indicated. The blue dashed line is a fit to the EQE data based on Varshni's law, with parameters from literature [16], which allows an estimation of the lowest transition energy at 0 K. The grey shaded area is a guide to the eye, indicating the expected range of E_g/q. The experimental uncertainty in V_{oc} and E_g/q is on the order of mV and therefore not shown.

$$\zeta = \sqrt[3]{\frac{\Delta_1 \pm \sqrt{\Delta_1^2 - 4\Delta_0^3}}{2}}, \tag{4a}$$

$$n = -\frac{1}{3C}(B + \zeta + \frac{\Delta_0}{\zeta}), \tag{4b}$$

and finally

$$V_{oc} = \frac{E_g}{q} + \frac{2k_BT}{q} \ln\left[-\frac{1}{3C\sqrt{N_cN_v}}(B + \zeta + \frac{\Delta_0}{\zeta})\right]. \tag{4c}$$

In (4a), the physically meaningful root must insure that n is real and positive. There is only one such root since $A, B, C, G > 0$. For evaluating E_g, we used the measured PL peak energy and the extrapolation to 0 K via Varshni's law. G in each QW was estimated from the measured short-circuit current density J_{sc} and EQE as $G = J_{sc}/(0.6N_{QW})$. $N_{QW} = 30$ is the number of QWs and 0.6 is a rough estimate for the extraction efficiency, which for simplicity has been taken as constant. The 2D densities of states in the QWs are given

by $N_{c,v} = m_{e,h}k_BT/\pi\hbar^2$, where we used for the effective masses m_e and m_h values from Ref. [16]. Table 1 lists all parameters and references.

At this point, it would be tempting to fit the parameters A, B and C to the data. This, however, does not solve the problem of the overestimation of E_g at $T = 0$ K. In addition, it leads to unreasonably high values of B and C compared to their published values [22, 23, 18]. Note, however, that a large C parameter might be justified in the case of carrier leakage, although this is observed in LEDs only at high carrier injection [20]. A large B parameter, on the other hand, could be justified by supposing a trap-assisted Auger process, but signatures of this have so far been observed only in low-efficiency MBE-grown devices [24]. Since values for B and C are relatively well established, both from measurements and theoretical predictions, we preferred to reduce the number of fitting parameters by using experimentally-extracted B and C from the work of Ref. [22]. Moreover, it is reasonable to assume that B and C have similar values in quantum wells of similar composition and thickness, as is the case here, while A may be largely process dependent.

In order to reproduce the observed thermal behavior, we adopted a temperature dependent model for A of the form [25, 26]

$$A(T) = \frac{A_0}{1 + \cosh(E_T/k_BT)}, \tag{5}$$

where A_0 in s^{-1} is a constant depending on defect density and properties of the defect state, and E_T is the energy level of the defect state measured from the intrinsic Fermi level. Figure 2 shows $A(T)$ for the parameters used in this work to fit the experimental V_{oc} (see Table 1) in comparison with published values [22] and the corresponding fit. It can be observed from the figure that the model can reasonably fit the measured $A(T)$ from [22], however with different parameters. The larger A_0 in our case suggests a larger trap density in the studied solar cell structures, while in both cases the obtained E_T indicates a deep trap level. E_T controls the slope of $A(T)$ at high temperatures, and in our analysis it is mainly responsible for the good simultaneous fit at all temperatures. We note, however, that using $E_T = 60$ meV instead of 120 meV does not dramatically change the results (see Supporting Information, Fig. S1). Also, our fitting parameters are not necessarily to be associated with a specific trap state, because they most probably have to be interpreted as effective parameters due to the phenomenological nature of our model.

Based on the measured short-circuit currents (see Supporting Information, Fig. S2), it is reasonable to expect that at 1000 suns carrier injection is still roughly an order of magnitude below that at typical current densities at maximum internal quantum efficiency in InGaN/GaN LEDs [18, 27]. Hence even at high solar concentration V_{oc} is still largely limited by SRH recombination. This holds true also when extrapolating the temperature dependence of B and C reported in Ref. [22] by a power law (see Supporting Information, Fig. S3), so that in our model we considered constant values for simplicity. Therefore, the measured change in slope of the V_{oc} versus intensity curves apparently cannot be explained by the transition between dominant recombination mechanisms.

Instead, we posit a non-negligible thermal effect, because under open circuit a major part of the absorbed optical power is transformed to heat via thermalization and non-radiative recombination of photogenerated charge carriers. The heat sink we used to maintain the cell at a constant base-plate temperature T cannot remove this heat fast enough to prevent noticeable cell overheating once the cell irradiance exceeds several hundred suns. To model this, we assumed a constant thermal resistance R_{Th} so that the device temperature is given by $T_{MQW} = T + R_{Th}P$, where P is the absorbed power. Using $P = 0.1$ W/cm^2 (1 sun) and the active cell area of 0.125×0.125 cm^2, we obtain $R_{Th} \approx 17$ K/W. This value is in the range that would be expected for our experimental configuration [28], and leads to an additional temperature increase of ~ 27 K at 1000 suns.

3. Results and Discussion

Figure 1 presents the modeled V_{oc} as a function of T and a broad range of solar intensities up to ~ 1000 suns together with our measurements, using model parameters given in Table 1. Data at higher intensities are not shown, because they are indistinguishable from the curve at 991 suns on the scale of the plot. The linear regression of the measured data and the extrapolation to 0 K are given by the red dashed lines. Since the measured qV_{oc} is expected to be smaller than E_g, or more specifically the ground-state transition

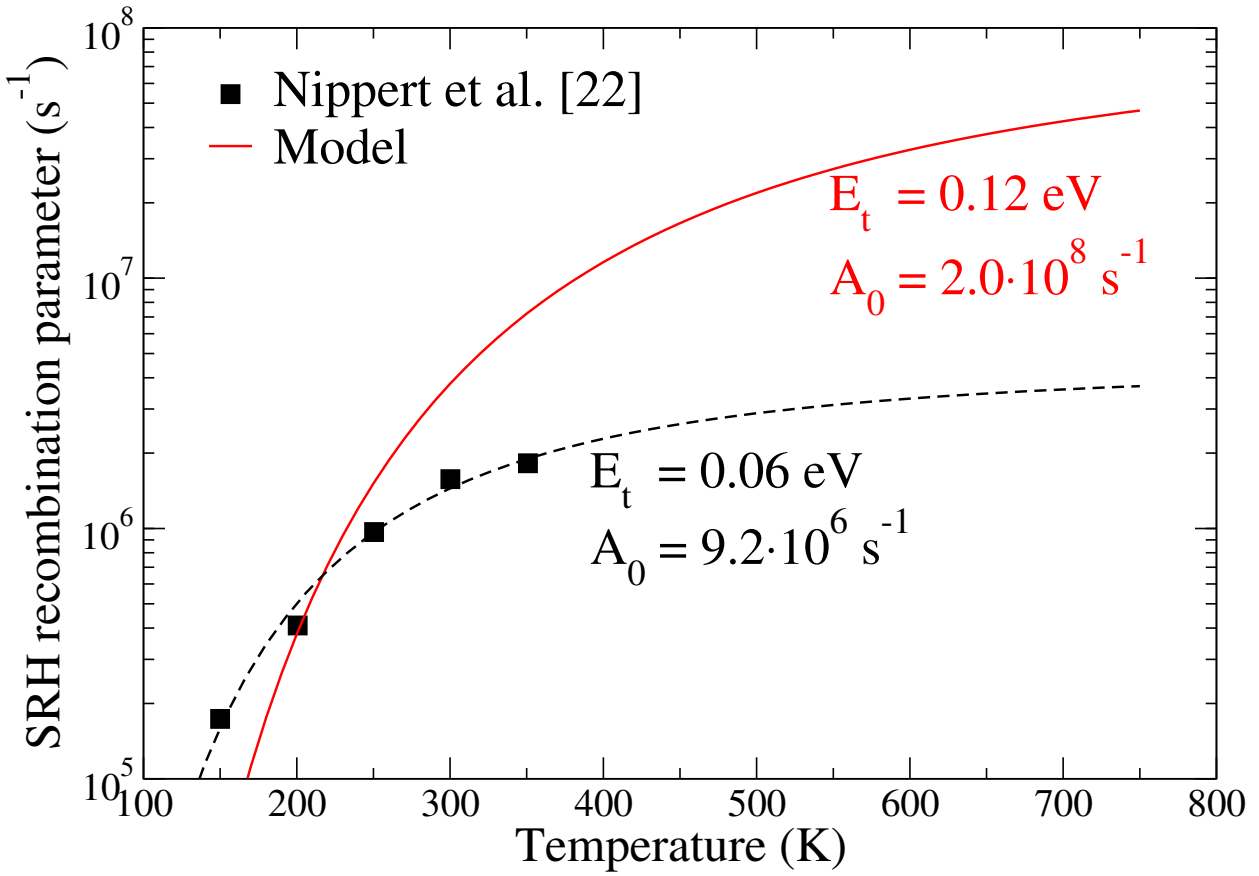

Figure 2: Temperature dependence of the SRH recombination parameter A according to Eq. (5), for the parameters used in this work (red). The symbols show values from Ref. [22], where A has been extracted from differential lifetime measurements (experimental uncertainty was not provided). The fit to Eq. (5) (dashed line) and corresponding parameters are given for comparison.

Table 1
Model parameters

Parameter	Value	Units	Source
A_0	$2 \cdot 10^8$	s^{-1}	Fit
E_T	0.12	eV	Fit
B	$2 \cdot 10^{-5}$	$cm^2 s^{-1}$	[22]
C	$5 \cdot 10^{-18}$	$cm^4 s^{-1}$	[22]
E_g	2.85	eV	meas.
m_e	0.2	-	[16]
m_h	1.4	-	[16]
R_{Th}	17	K/W	Fit

energy, we compare it with the measured PL peak energy and E_g extracted from EQE measurements. This is indicated in Fig. 1 by the green star and the blue open symbols, respectively. In order to obtain E_g at 0 K, we extrapolated the data according to Varshni's law for the temperature dependence of E_g, using published values for the model parameters and a linear interpolation between values for GaN and InN [16].

The linear interpolation from the high-temperature V_{oc} data leads to an overestimation of E_g which is incompatible with the direct measurement. Moreover, this precludes fitting the data using the measured E_g. In contradistinction, it can be seen that the model employing a temperature-dependent SRH parameter

A predicts a change in slope at around 200 K, which is associated with a transition from SRH to radiative-dominated recombination. Setting E_g in the analytic formulas to the value obtained by measurement, we can consistently reproduce the measurements using the correct E_g at 0 K. This shows that incorrect values of E_g are obtained from linear regression of the data around room temperature due to the temperature dependence of the recombination parameters. Moreover, such a transition to a radiatively-dominated regime at low temperatures is compatible with the assumption often made for III-nitride LEDs that the PL efficiency approaches 100% near 0 K [29].

Figure 3 compares model results against the data as a function of intensity. The slope of 2 at low solar concentration is well reproduced, while the sub-linear behavior at larger concentration is accounted for by the additional heating as described above. Note that the curves at different temperatures can be fitted conjointly thanks to the temperature dependent model for the SRH parameter. Trying to reproduce these curves by adjusting the recombination parameters A, B and C is possible, but leads to values of B and C which are up to 5 orders of magnitude larger than published values (vide supra). In fact, in the devices studied here, Auger recombination does not seem to be relevant and could therefore have been eliminated from Eq. (3). However, in view of its application to other solar cell types and materials, we find it preferable to formulate the model including all three main recombination models.

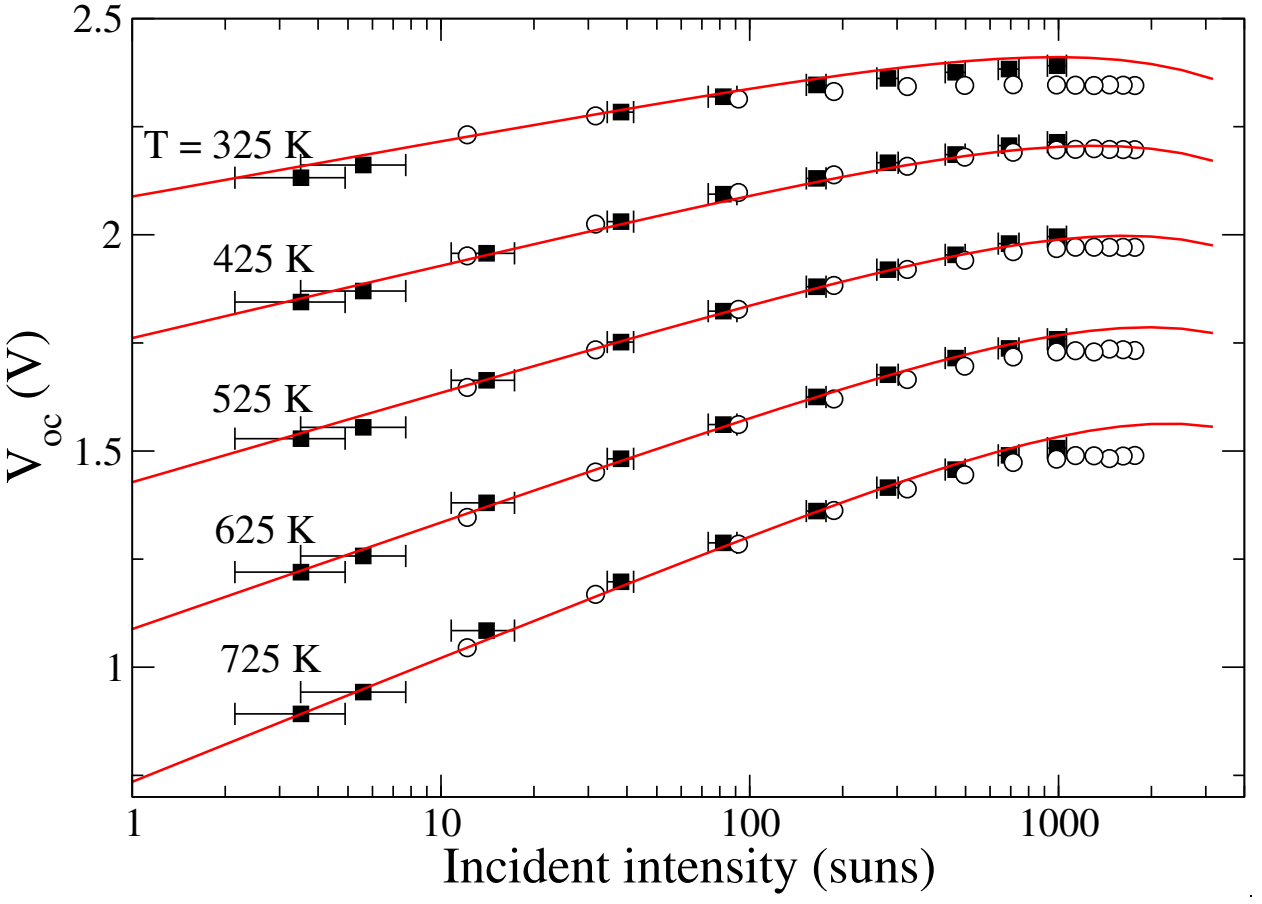

Figure 3: V_{oc} versus solar intensity for the studied cell at different base plate temperatures. The solid black squares and open white circles are values measured on the same device on two different days. The red lines are model predictions as described in the text. The change in slope can be explained by self-heating of the cell under high intensity. Experimental uncertainty in intensity is indicated for one of the data sets.

4. Conclusions

In conclusion, we have shown that the measured intensity and temperature dependence of V_{oc} of c-plane InGaN/GaN MQW solar cells is compatible with the ABC model describing recombination in such structures, provided a temperature-dependent SRH parameter is used and self-heating is taken into account. The model can then correctly reproduce the high temperature behavior of V_{oc}, while recovering the correct value of E_g at 0 K. The results also explain the discrepancy between the linear temperature extrapolation of V_{oc} to 0 K and the measured E_g. This is important inasmuch as V_{oc} at 0 K represents the maximum voltage that can be generated by a solar cell. In this context, it will be interesting to generalize our results to a wide range of solar cells based on direct and indirect semiconductors.

Acknowledgments

GM's doctoral fellowship was funded by Research Grant number 3-15970 from the Israel Ministry of Science, Technology and Space, as well as by Ben-Gurion University's Albert Katz International School for Desert Studies and the Hitech Biotech Scholarship from the University's Kreitman School of Advanced Graduate Studies.

CRediT authorship contribution statement

Matthias Auf der Maur: Formal analysis, Methodology, Visualization, Writing - Original draft preparation. **Gilad Moses:** Investigation, Writing - review & editing. **Jeffrey M. Gordon:** Conceptualization, Supervision, Writing - review & editing. **Xuanqi Huang:** Resources, Writing - review & editing. **Yuji Zhao:** Resources, Writing - review & editing. **Eugene A. Katz:** Conceptualization, Supervision, Resources, Writing - review & editing.

References

[1] R. Dahal, B. Pantha, J. Li, J. Y. Lin, H. X. Jiang, InGaN/GaN multiple quantum well solar cells with long operating wavelengths, Applied Physics Letters 94 (2009) 063505.

[2] A. G. Bhuiyan, K. Sugita, A. Hashimoto, A. Yamamoto, InGaN solar cells: Present state of the art and important challenges, IEEE Journal of Photovoltaics 2 (2012) 276–293.

[3] J. J. Williams, H. McFavilen, A. M. Fischer, D. Ding, S. Young, E. Vadiee, F. A. Ponce, C. Arena, C. B. Honsberg, S. M. Goodnick, Refractory In_x Ga_{1-x} N Solar Cells for High-Temperature Applications, IEEE Journal of Photovoltaics 7 (2017) 1646–1652.

[4] J.-H. Park, R. Nandi, J.-K. Sim, D.-Y. Um, S. Kang, J.-S. Kim, C.-R. Lee, A III-nitride nanowire solar cell fabricated using a hybrid coaxial and uniaxial InGaN/GaN multi quantum well nanostructure, RSC Adv. 8 (2018) 20585–20592.

[5] J. Bai, Y. Gong, Z. Li, Y. Zhang, T. Wang, Semi-polar InGaN/GaN multiple quantum well solar cells with spectral response at up to 560nm, Solar Energy Materials and Solar Cells 175 (2018) 47–51.

[6] X. Huang, H. Chen, H. Fu, I. Baranowski, J. Montes, T.-H. Yang, K. Fu, B. P. Gunning, D. D. Koleske, Y. Zhao, Energy band engineering of InGaN/GaN multi-quantum-well solar cells via AlGaN electron- and hole-blocking layers, Applied Physics Letters 113 (2018) 043501.

[7] X. Huang, W. Li, H. Fu, D. Li, C. Zhang, H. Chen, Y. Fang, K. Fu, S. P. DenBaars, S. Nakamura, S. M. Goodnick, C.-Z. Ning, S. Fan, Y. Zhao, High-Temperature Polarization-Free III-Nitride Solar Cells with Self-Cooling Effects, ACS Photonics 6 (2019) 2096–2103.

[8] G. Moses, X. Huang, Y. Zhao, M. Auf der Maur, E. A. Katz, J. M. Gordon, InGaN/GaN multi-quantum-well solar cells under high solar concentration and elevated temperatures for hybrid solar thermal-photovoltaic power plants, Progress in Photovoltaics: Research and Applications 28 (2020) 1167–1174.

[9] J. Zeitouny, N. Lalau, J. M. Gordon, E. A. Katz, G. Flamant, A. Dollet, A. Vossier, Assessing high-temperature photovoltaic performance for solar hybrid power plants, Solar Energy Materials and Solar Cells 182 (2018) 61–67.

[10] A. Braun, E. A. Katz, J. M. Gordon, Basic aspects of the temperature coefficients of concentrator solar cell performance parameters, Progress in Photovoltaics: Research and Applications 21 (2013) 1087–1094.

[11] M. Auf der Maur, A. Di Carlo, Analytic approximations for solar cell open circuit voltage, short circuit current and fill factor, Solar Energy 187 (2019) 358 – 367.

[12] O. Dupré, R. Vaillon, M. A. Green, Thermal Behavior of Photovoltaic Devices, Springer International Publishing AG, Gewerbestrasse 11, 6330 Cham, Switzerland, 2017.

[13] M. Auf der Maur, B. Galler, I. Pietzonka, M. Strassburg, H. Lugauer, A. Di Carlo, Trap-assisted tunneling in InGaN/GaN single-quantum-well light-emitting diodes, Applied Physics Letters 105 (2014).

[14] E. A. Katz, J. M. Gordon, D. Feuermann, Effects of ultra-high flux and intensity distribution in multi-junction solar cells, Progress in Photovoltaics: Research and Applications 14 (2006) 297–303.

[15] J. M. Gordon, E. A. Katz, D. Feuermann, M. Huleihil, Toward ultrahigh-flux photovoltaic concentration, Applied Physics Letters 84 (2004) 3642–3644.
[16] I. Vurgaftman, J. Meyer, L. Ram-Mohan, Band parameters for nitrogen-containing semiconductors, Applied Physics Review 94 (2003) 3675–3696.
[17] S. Karpov, ABC-model for interpretation of internal quantum efficiency and its droop in III-nitride LEDs: a review, Optical and Quantum Electronics 47 (2015) 1293–1303.
[18] A. David, N. G. Young, C. Lund, M. D. Craven, Review—the physics of recombinations in III-nitride emitters, ECS Journal of Solid State Science and Technology 9 (2020) 016021.
[19] S. M. Sze, Semiconductor Devices: Physics and Technology, John Wiley & Sons, New York, 1985.
[20] J. Piprek, How to decide between competing efficiency droop models for GaN-based light-emitting diodes, Applied Physics Letters 107 (2015) 031101.
[21] R. Nickalls, A new approach to solving the cubic: Cardan's solution revealed, The Mathematical Gazette 77 (1993) 354–359.
[22] F. Nippert, S. Y. Karpov, G. Callsen, B. Galler, T. Kure, C. Nenstiel, M. R. Wagner, M. Straßburg, H.-J. Lugauer, A. Hoffmann, Temperature-dependent recombination coefficients in InGaN light-emitting diodes: Hole localization, Auger processes, and the green gap, Applied Physics Letters 109 (2016) 161103.
[23] R. Zhou, M. Ikeda, F. Zhang, J. Liu, S. Zhang, A. Tian, P. Wen, D. Li, L. Zhang, H. Yang, Total-InGaN-thickness dependent Shockley-Read-Hall recombination lifetime in InGaN quantum wells, Journal of Applied Physics 127 (2020) 013103.
[24] A. C. Espenlaub, D. J. Myers, E. C. Young, S. Marcinkevičius, C. Weisbuch, J. S. Speck, Evidence of trap-assisted Auger recombination in low radiative efficiency MBE-grown III-nitride LEDs, Journal of Applied Physics 126 (2019) 184502.
[25] C. D. Santi, M. Meneghini, D. Monti, J. Glaab, M. Guttmann, J. Rass, S. Einfeldt, F. Mehnke, J. Enslin, T. Wernicke, M. Kneissl, G. Meneghesso, E. Zanoni, Recombination mechanisms and thermal droop in AlGaN-based UV-B LEDs, Photon. Res. 5 (2017) A44–A51.
[26] A. Rashidi, M. Monavarian, A. Aragon, D. Feezell, Thermal and efficiency droop in InGaN/GaN light-emitting diodes: decoupling multiphysics effects using temperature-dependent RF measurements, Scientific Reports 9 (2019).
[27] I. Reklaitis, L. Krencius, T. Malinauskas, S. Y. Karpov, H. J. Lugauer, I. Pietzonka, M. Strassburg, P. Vitta, R. Tomašiūnas, Time of carrier escape and recombination coefficients in InGaN quantum-well active regions of blue, cyan, and green light-emitting diodes, Semiconductor Science and Technology 34 (2018) 015007.
[28] J. Sun, T. Israeli, T. A. Reddy, K. Scoles, J. M. Gordon, D. Feuermann, Modeling and Experimental Evaluation of Passive Heat Sinks for Miniature High-Flux Photovoltaic Concentrators , Journal of Solar Energy Engineering 127 (2005) 138–145.
[29] S. Watanabe, N. Yamada, M. Nagashima, Y. Ueki, C. Sasaki, Y. Yamada, T. Taguchi, K. Tadatomo, H. Okagawa, H. Kudo, Internal quantum efficiency of highly-efficient $In_xGa_{1-x}N$-based near-ultraviolet light-emitting diodes, Applied Physics Letters 83 (2003) 4906–4908.